Geophysical Research Letters

Key Points:

- The first study to investigate the potential impact of topography of Tibetan Plateau (TP) on the formation of the Antarctic bottom water (AABW)
- Removing the TP can enhance AABW circulation via fast atmosphere teleconnections and subsequent slow ocean adjustments
- The Weddell Sea is responsible for the initial AABW strengthening while the Bellingshausen Sea plays a sustaining role

Supporting Information:

- Supporting Information S1

Correspondence to:

Q. Wen and H. Yang,
wenq@pku.edu.cn;
yanghj@fudan.edu.cn

Can the Topography of Tibetan Plateau Affect the Antarctic Bottom Water?

Qin Wen[1] , Chenyu Zhu[2], Zixuan Han[3] , Zhengyu Liu[4], and Haijun Yang[5]

[1]School of Geography, Key Laboratory of Virtual Geographic Environment(Nanjing Normal University), Ministry of Education, Jiangsu Center for Collaborative Innovation in Geographical Information Resource Development and Application, Nanjing, China, [2]Key Laboratory of Physical Oceanography, Ocean University of China, Open Studio for Ocean-Climate-Isotope Modeling, Pilot National Laboratory for Marine Science and Technology, Qingdao, China, [3]College of Oceanography/Key Laboratory of Marine Hazards Forecasting, Ministry of Natural Resources/ Key Laboratory of Ministry of Education for Coastal Disaster and Protection, Hohai University, Nanjing, China, [4]Department of Geography, Ohio State University, Columbus, OH, USA, [5]Department of Atmospheric and Oceanic Sciences, Institute of Atmospheric Science and CMA-FDU Joint Laboratory of Marine Meteorology, Fudan University, Shanghai, China

Abstract The Tibetan Plateau (TP) plays a vital role in shaping global climate. So far, however, few studies have focused on the impact of the TP on Southern Ocean (SO) circulation. Through fully coupled model experiments with and without the TP, we find that removing the TP could eventually enhance Antarctic bottom water (AABW) circulation by generating Rossby wave trains that propagate from the tropical Indo-Pacific to Amundsen-Bellingshausen Sea. The surface air temperature (SAT) cools over the Antarctic Peninsula, which then leads to increased brine injection and thus the initial enhancement of AABW. Later on, the increased horizontal salinity transport and oceanic vertical mixing over Bellingshausen Sea further strengthen the AABW. These findings imply that long term changes of AABW can be affected by not only local process but also remote forcing, including those from the Asian highland regions.

Plain Language Summary To understand how the topography of the Tibetan Plateau (TP) may affect Antarctic bottom water (AABW) circulation, we conduct model experiments with and without the TP. We find that removing the TP can enhance the AABW circulation via fast atmosphere teleconnections and subsequent slow ocean adjustments. The TP removal immediately generates a Rossby wave train from Indo-Pacific to reach at Antarctic coast, resulting in anomalous low-pressure system over Weddell Sea (WS) and high-pressure system over Amundsen-Bellingshausen Sea. The former causes surface air cooling and increases brine injection over WS, which is responsible for the initial AABW strengthening. The latter weakens the westerlies and enhances the southward Ekman transport, which brings saltier water to Bellingshausen Sea. This process takes effect after 600 years and, accompanied by enhanced vertical salinity diffusion, leads to re-enhancement of AABW circulation. Our study implies that long term changes of AABW can be affected by not only local process but also remote forcing, even those from the Asian highland regions.

1. Introduction

With an average elevation of more than 4,000 m above the sea level and an area of 2.5 million square kilometers, the Tibetan Plateau (TP) plays a crucial role in the formation of modern climate. It exerts enormous dynamic and thermal impacts on weather and climate not only in Asia (An et al., 2001; Boos & Kuang, 2010; Kutzbach et al., 1989; Wu et al., 2012), but also remotely in the North America through planetary waves (Held & Ting, 1990; Hoskins & Karoly, 1981; Zhou et al., 2009). The uplift of the TP began about 50 Myr (million years) ago, and accelerated about 10–8 Myr ago (Harrison et al., 1992; Molnar et al., 1993). This uplift has been suggested to have enhanced the Indian and East Asian monsoon, the aridity in the Eurasian interior, the westerly jet stream in winter in the Northern Hemisphere (Ruddiman & Kutzbach, 1989), and the dust transport to the North Pacific Ocean (An et al., 2001).

The global ocean circulation is likely affected by tectonic changes since Eocene, in, for example, the Drake Passage (e.g., Pfister et al., 2014), Bering Strait (e.g., Hu et al., 2015) and mountain uplift (e.g., Yang &

Wen, 2020). The effects of orography on oceanic properties emerge as an important issue in recent years to understand the formation of modern ocean circulations (Fallah et al., 2016; Kitoh, 1997; Wen & Yang, 2020; Yang & Wen, 2020). Many studies show that the present-day configuration of high mountains forces the thermohaline circulation toward its modern state, that is, deep-water formation in the North Atlantic, whereas it tends to occur in the Pacific in a flat world (Schmittner et al., 2011; Sinha et al., 2012). Recent studies of Su et al. (2018), Yang and Wen (2020), as well as Wen and Yang (2020) have attributed these changes to the TP. So far, however, few studies have focused on the impact of the TP on the Southern Ocean (SO) circulation, particularly, the Antarctic bottom water (AABW).

Today, AABW is the coldest and densest water mass and occupies most of the world's deep basins, ventilating the lower limb of the meridional overturning circulation (MOC) (Johnson, 2008; Lumpkin & Speer, 2007). The modulation of AABW strength is important for global heat and sea level rise budgets (Kouketsu et al., 2011; Purkey & Johnson, 2013), air-sea gas exchange and atmospheric CO_2 concentrations (Stephens & Keeling, 2002). The AABW has been suggested to be affected by various mechanisms, including the mixing process and density distribution in the deep ocean (Kamenkovich & Goodman, 2000), eddies in the circumpolar channel (Ito & Marshall, 2008; Nikurashin & Vallis, 2011). Now, buoyancy flux lies at the heart of the AABW response under external forcings, in which the sea ice formation and associated brine injection in the SO plays a major role (Adkins et al., 2013; Ferrari et al., 2014; Shin et al., 2003; Sun et al., 2016). For example, based on ocean state estimates and coupled climate model results, Ferrari et al. (2014) show that the sea ice extent around Antarctic during Last Glacial Maximum exerts a strong control on the surface buoyancy flux in the SO, and thus the AABW circulation. The analytical results of Steward et al. (2014) also suggest a sensitivity of the abyssal circulation to buoyancy loss around Antarctica. Building on these previous works, Jansen and Nadeau (2016) systematically analyze the role of both the meridional extent of buoyancy loss around Antarctica as well as the rate of buoyancy loss. Their results highlight the importance of the integrated buoyancy loss rate around Antarctica.

Thus, how the topography of the TP affects the buoyancy flux over SO? How AABW responds in a world without the TP? This is a very interesting question that has never been addressed before. Investigating the role of the TP in AABW changes may help us understanding the long-term climate changes in the past and may also have implications to climate changes in the future. Simulations with a state-of-the-art Community Earth System Model(CESM) allow us to see more clearly the signals and mechanisms in both local and remote regions associated with forcing factors.

2. Model and Simulations

The CESM1.0 is employed in this study. This is a fully coupled global climate model with dynamic atmosphere, land, ocean, sea ice components and one coupler, developed by the U.S. National Centre for Atmospheric research (NCAR) (Hunke & Lipscomb, 2010; Lawrence et al., 2012; Park et al., 2014). It has been widely used and validated to study the Earth's past, present, and future climate (e.g., Hurrell et al., 2013; Yang et al., 2015). We choose the low-resolution configuration: the horizontal grid of atmospheric model (CAM5) is roughly 3.75° × 3.75° (T31) with 26 vertical levels. The land model (CLM4) has the same horizontal resolution as the CAM5. The ocean model (POP2) adopts a finer oceanic horizontal grid, with 60 vertical levels, a uniform 3.6° spacing in the zonal direction, and a non-uniformly spacing in the meridional direction: It is 0.6° near the equator, gradually increasing to the maximum 3.4° at 35°N/S and then decreasing poleward. The sea ice model (CICE4) has the same horizontal grid as the POP2. No flux adjustments are used in CESM1.0.

Two experiments are conducted to investigate the TPs role in shaping AABW strength. The first experiment is CTRL, in which the modern topography is used (Figure S1a). The CTRL simulation uses standard configuration with a preindustrial CO_2 concentration of 285 ppm. The simulation is integrated for 1,500 years to reach the equilibrium state (Yang et al., 2015) and is integrated for additional 400 years for comparison with the second experiment. This second experiment is the sensitivity experiment without the TP (NoTP), in which the topography of the TP is reset to 50 m above the sea level (Figure S1b). The NoTP simulation starts from the year 1501 of CTRL and is integrated for 1,400 years. Except for topography, all other boundary conditions, including land-sea distribution and CO_2 concentration remain the same as that in CTRL.
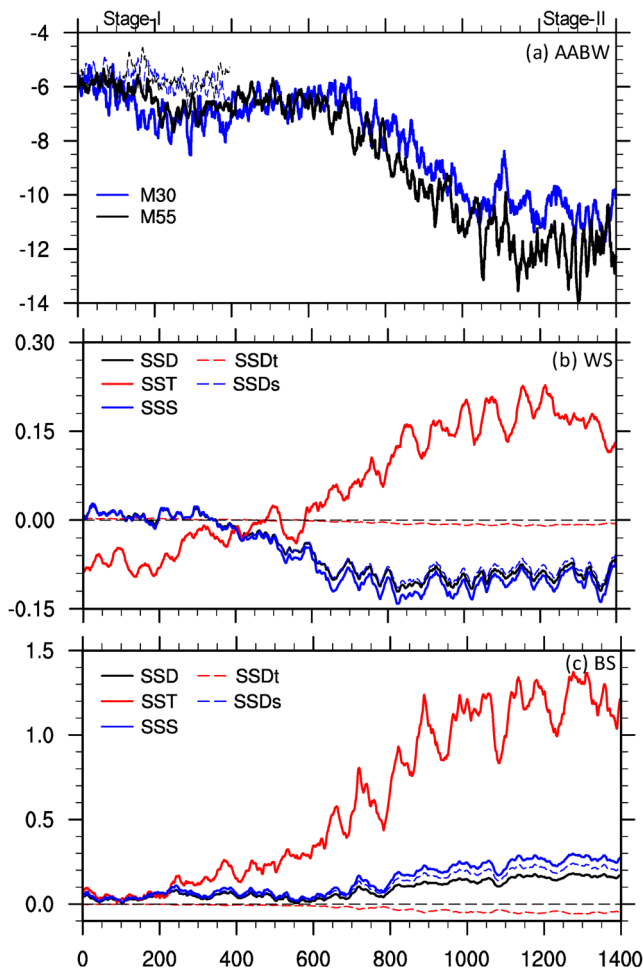
Figure 1. (a) Temporal evolution of Antarctic bottom water (AABW) circulation. The black curve represents the south AABW index which is defined as the minimum stream function south of 55°S in the Southern Ocean (M55) while the blue curve represents the north AABW index which is defined as the minimum stream function north of 30°N under 2,000 m depth (M30). These two regions are outlined by black dashed rectangles in Figure S2a. Units: Sv. 1 Sv = 10^9 kg/m³. Stage-I is 50–250 years, Stage-II is 1,300–1,400 years. The solid curves are for the values in NoTP while dashed curves are for CTRL. (b) Temporal changes in SSD (black; kg/m³), SST (red; °C), and SSS (blue; psu) over Weddell Sea. The SSD changes due to SSS and SST are plotted as dashed thin blue and red curves, respectively. (c) is the same as (b) but for Bellingshausen Sea.

The planetary albedo can adjust by itself according to thermal conditions. The AABW change due to the TP removal is obtained by subtracting the results of CTRL from those of NoTP.

We define two kinds of AABW index here to ensure the robust change in abyssal ocean circulation. The south AABW index (M55) is defined as the minimum stream function in the range of 0–4,000 m over 55°–80°S (outlined by dashed rectangle in Figure S2a), which is directly linked to SO surface forcing and represents the shallow AABW circulation. The north AABW index (M30) is defined as the minimum stream function in the range of 2,600–5,000 m over 30°S northward (outlined by dashed rectangle in Figure S2a), representing the abyssal ocean circulation.

3. Results

3.1. AABW Response

Before showing the AABW response to the TP removal, we want to repeat that removing the TP can lead to Atlantic meridional overturning circulation (AMOC) shutdown and Pacific meridional overturning circulation (PMOC) establishment (Figure S3). The mechanisms for AMOC and PMOC response have been carefully examined in our previous works (Wen & Yang, 2020; Yang & Wen, 2020). The weakened AMOC can generate bipolar seesaw temperature distribution with cooling in the North Atlantic and warming in the South Atlantic (Figures S4a and S4g) (Delworth & Zeng, 2012). In addition, the shutdown of AMOC promotes cold and fresh surface water in the North Atlantic penetrating downward, and southward along the western boundary current to reach the SO (Figures S4a, S4b, S4g, S4h). Then, it joins the Antarctic Circumpolar Current and transports eastward to reach Pacific section (Figure S5). This path is described by classical ocean circulation theory (Talley, 2013). These mean climate changes are important for our later study of AABW. The time evolution of two kinds of AABW index are shown in Figure 1a. In CTRL simulation, the AABW strength is about 6 Sv, which is lower than the observed estimates (21 ± 6 Sv) suggested by Ganachaud and Wunsch (2001) but comparable with other model values (i.e., Zhang et al., 2017). The evolution of M55 and M30 are highly consistent with each other, with the maximum correlation coefficient of 0.94 occurred when M55 leads M30 by 15 years (Figure not shown). This lead of south AABW index to north AABW index is easy to understand: the AABW forms in confined regions around Antarctica and takes time for mixing and transporting northward into different basins (Sebille et al., 2013). Both the north and south AABW indices show a slow and modest increase of the AABW during the first 250 years, a gradual reduction to its CTRL strength between 250 and 600 years, and a rapid intensification after 600 years. Since the AABW does not change linearly, the mechanisms may be different during different stages. For the convenience of discussion, we define two stages according to the evolution of the AABW index: Stage-I is from model year 50 to year 250 when initial AABW strengthening is occurred, and Stage-II is from model year 1300 to year 1400 representing the equilibrium stage.

3.2. Buoyancy Response

AABW source water is closely related to surface buoyancy lose over regions around Antarctic (Snow et al., 2016). In our study, the key regions for generating AABW change is Weddell Sea (WS) and Bellingshausen Sea (BS) based on abyssal ocean density outcrop regions during austral winter (Figures S6a and S6d). The
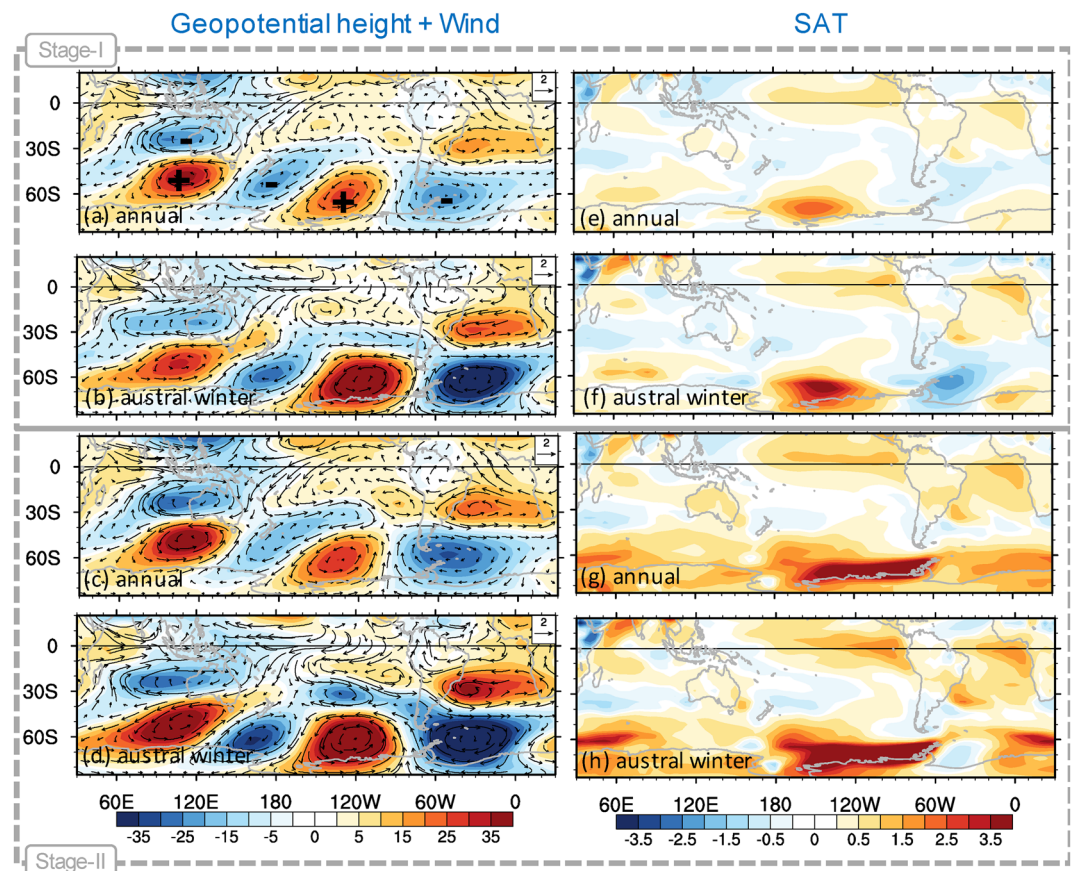
Figure 2. Changes in (a–d) eddy geopotential height (shading; units: m) and wind (vector; units: m/s) at 200 hPa and (e–h) surface air temperature (SAT; °C). (a, e, c, and g) are for annual mean. (b, f, d, and h) are for austral winter.

outcrop region is the place where surface water is dense enough to form the AABW. Note that the AABW is formed during austral winter and the abyssal ocean density outcrops at the surface during this season. Moreover, the buoyancy condition during austral winter is closely related to its annual mean value. To understand regional mechanisms related to AABW change, the temporal evolution of annual mean sea surface density (SSD), sea surface salinity (SSS) and sea surface temperature (SST) over WS and BS are first examined in Figures 1b and 1c. In WS, the SSD is nearly unchanged during the first several hundred years, and then decreased substantially due to surface freshening (black and blue curves in Figure 1b). The surface warming (red curve in Figure 1b) melts the sea ice and freshens the surface ocean (Figure S7a). The SSD reduction leads to the shrinking of outcrop region (Figure S6). In BS, the SSD gradually rises and is increased by 0.2 kg/m³ by the end of Stage-II due to surface salinization (black and blue curves in Figure 1c). The salinity budget over this region shows that the advection and mixing processes contribute to the SSS increase (Figure S7b). In contrast to WS, the SSD increase over BS leads to the expansion of outcrop region (Figure S6), indicating the BS as an additional candidate region for AABW formation.

3.3. Mechanisms

3.3.1. Atmospheric Response

The influence of the TP on AABW circulation is via adjustment of atmospheric circulation. Removing the TP immediately leads to a positive Indian Ocean dipole-like SST pattern over the Indian Ocean and El Niño-like SST pattern over the tropical Pacific Ocean (Figure S8c). The SST change over the Indian Ocean and the Pacific Ocean is caused by weakened climatological southerly wind over the Indian Ocean and trade wind over the Pacific Ocean (Figure S8b). The Indian Ocean and Pacific Ocean SST changes generate a wave-5 pattern over SO (Figure 2) resulting in anomalous high-pressure over Amundsen Sea and low-pressure over

WS. Actually, the atmospheric teleconnection between the tropical Indo-Pacific and Antarctica has been studied extensively (Nuncio & Yuan, 2015; Purich & England, 2019; Wang et al., 2019). The wave-5 pattern obtained in our study is overall consistent with earlier results. However, there are also some differences. For example, the magnitude of Rossby wave in our study is much stronger and displaced much poleward than the results from Nuncio & Yuan (2015; their Figure 3c) and Wang et al. (2019; their Figure 3d). In addition, by conducting an Indo-Pacific pacemaker experiment, Purich & England (2019) only get wave-3 (their Figure S1) although the observation data in their study shows a wave-5 pattern (their Figure 1). These differences are understandable since the SST pattern in our study is not exactly the same as that in previous works and the atmospheric process may also play a role in shaping the final structure of Rossby waves (Turner 2004). The atmospheric responses in our study are roughly barotropic in high latitudes because the changes at 200 and 850 hPa are similar to each other (Figure not shown). The wave structure is similar during the two stages and the magnitude in Stage-II is stronger than that in Stage-I (Figure 2c vs. Figure 2a). The Rossby wave over SO weakens the westerlies and southern annular mode (Figure S11a). The wave train is further strengthened and shifts eastward during austral winter, resulting in anomalous southerly winds over Antarctic Peninsula and its surrounding regions (Figures 2b and 2d). In Stage-I when oceanic process does not fully respond, the anomalous southerly winds over the Antarctic Peninsula brings cold air from polar regions northward, cooling the surface air over the WS and the eastern BS (Figures 2e and 2f). In contrast, the anomalous northerly winds over the western Amundsen Sea bring relatively warm air from lower latitudes, resulting in warm surface air temperature (SAT) there (Figures 2e and 2f). The out-of-phase relationship of SAT between Pacific and Atlantic section of SO under SST forcing from tropic ocean has been revealed in prior works (Ding et al., 2011; Nuncio & Yuan, 2015). In Stage-II, because the ocean is fully adjusted, the SAT shows warm anomaly over most regions of SO, even over Antarctic Peninsula where the anomalous southerly winds can still bring cold air. We want to emphasize that the SAT cooling over WS during Stage-I is the triggering mechanism for AABW strengthening while the anomalous high-pressure over Amundsen Sea, which weakens the westerlies and drives anomalous southward Ekman transport (Figure 4), is the sustaining mechanism for AABW strengthening.

3.3.2. Ocean Dynamics

The WS is responsible for the initial enhancement of AABW circulation. In Stage-I, during which the SSD is nearly unchanged over WS (Figures 1b and S6a), the SAT cooling driven by atmospheric response is in favor of sea ice formation during austral winter, which increases the sea ice thickness, brine injection and thus the density flux (Figures 3a–3c, S9a and S9b). The increased density flux leads to buoyancy loss and thus strengthens the AABW formation during austral winter. After Stage-I, the annual mean SSD is reduced due to decreased SSS, which is primarily caused by SST warming (Figure 1b). The warmer SST melts the sea ice and increases the freshwater water import to ocean (Figure S7a). The reduction of SSS dominates the density change and thus makes AABW formation weakened, which leads to AABW reduction to its CTRL strength after Stage-I (Figure 1b).

The BS is responsible for the re-enhancement of AABW circulation after 600 years, with very different mechanisms compared with that in the WS depending on SSS change (Figure 1c). As suggested above, removing the TP generates the anomalous southerly winds and thus the SAT cooling over Antarctic Peninsula, which favors the sea ice formation and triggers the increase of SSS during the first 400 years. Later on, the horizontal advection and vertical mixing processes take effect (gray and blue curves in Figure S7b). The anomalous high pressure over Amundsen Sea weakens the westerlies since the anomalous easterlies exist around 45°S (Figure 2a). The weakened westerlies lead to anomalous southward Ekman transport (Figure S11b), manifested by anomalous southward ocean current in Figures 4b and 4d. This helps to bring saltier water from the western South Pacific to eastern BS (Figure 4b). This process takes effect after 600 years (Figure 4d) when profound high latitude warming at Pacific section further weakens the westerlies and strengthens the anomalous southward Ekman transport (Figure S11b). In addition, the weakened westerlies lead to a strengthening of the blocking effect of the Antarctic Peninsula orography (Marshall et al., 2006). The southwestward compensation flow near the Antarctica coast also helps to bring saltier water there. The vertical mixing effect is affected by water column stability. The surface water salinization due to local brine injection (red curve in Figure S7b) and salinity advection (blue curve in Figure S7b), and subsurface water freshening coming from North Atlantic (Figure S5) make water column unstable (negative stability; Figure S10b). The unstable water column leads to increased vertical convection and mixing, indicated by increased vertical
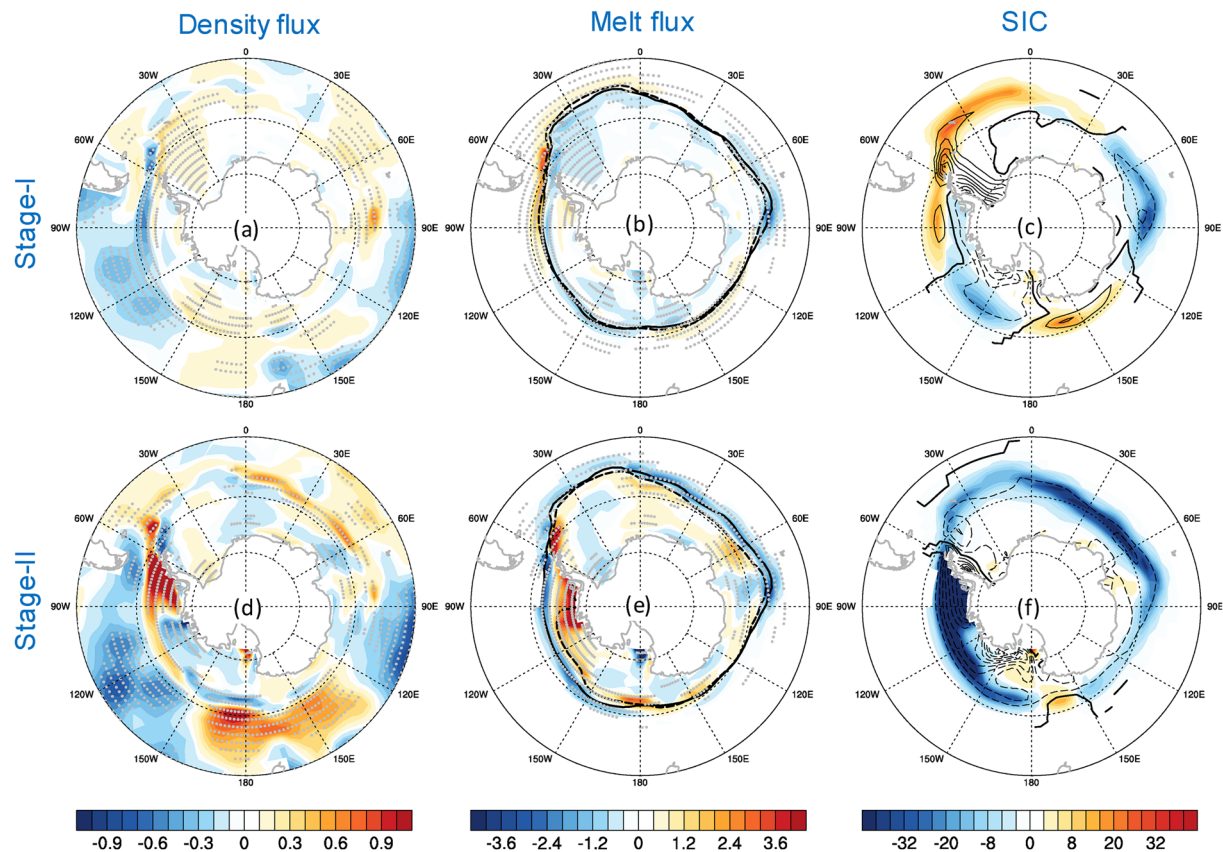
Figure 3. Changes in (a) density flux (10^{-6} kg/m^2/s); (b) melt flux (10^{-5} kg/m^2/s); (c) sea ice coverage (SIC; shading; units: %) and sea ice thickness (contour; units: m) during Stage-I. In (c), the solid black contours represent the positive sea ice thickness change while the dashed contours are for negative change. In (a, b, d, and e), the stippling indicates the 95% confidence level determined by a two-tailed Student's t-test. In (b and e), the solid and dashed black contours denote the sea ice margin defined by 15% sea ice coverage. Panels (d–f) are the same as (a–c) but for Stage-II. All these variables are from austral winter.

salinity diffusivity (Figure S10c), which in turn increases (decreases) the surface (subsurface) ocean salinity (Figures S7b and S10a). The annual mean SSS increase over Amundsen-Bellingshausen Sea provides a favorable condition for the AABW formation. The enhanced AABW then causes strong SST warming over the Amundsen-Bellingshausen Sea. The SST warming over this region leads to a dramatic sea ice retreat (Figure 3e), which exposes much seawater to lose heat directly to the atmosphere. When the sea-ice retreat is sufficiently large, the increased density flux by the heat loss could overwhelm the decreased from the SST warming, which could also potentially contribute to the AABW formation in NoTP at longer timescale (Figures S9c and S9d) (Zhu et al., 2015). The enhanced AABW formation over BS offsets the weakened AABW formation over WS after 600 years and finally results in AABW strengthening again (Figure 1b).

4. Conclusion and Discussion

In this study, we have explored the AABW response to TP removal through experiments with and without the TP and concluded that removing the TP would eventually enhance the AABW circulation. Removing the TP can generate a Rossby wave train excited from the tropical Indo-Pacific to reach at Antarctic coast, resulting in anomalous low-pressure over WS and high-pressure over Amundsen Sea. The former cools the WS, which increases the brine injection and thus the AABW strengthening during the first 250 years. The contribution from WS is weakened and disappeared at around 600 years, since the ocean surface warming induced by weakened AMOC (Liu & Fedorov, 2019) and enhanced AABW (Zhang et al., 2017) melts the sea ice and hinders the AABW formation there. The latter weakens the westerlies and triggers anomalous southward Ekman transport, which brings saltier water to BS. This process takes effect after 600 years and, accompanied by enhanced vertical salinity diffusion, leads to reenhancement of AABW circulation.
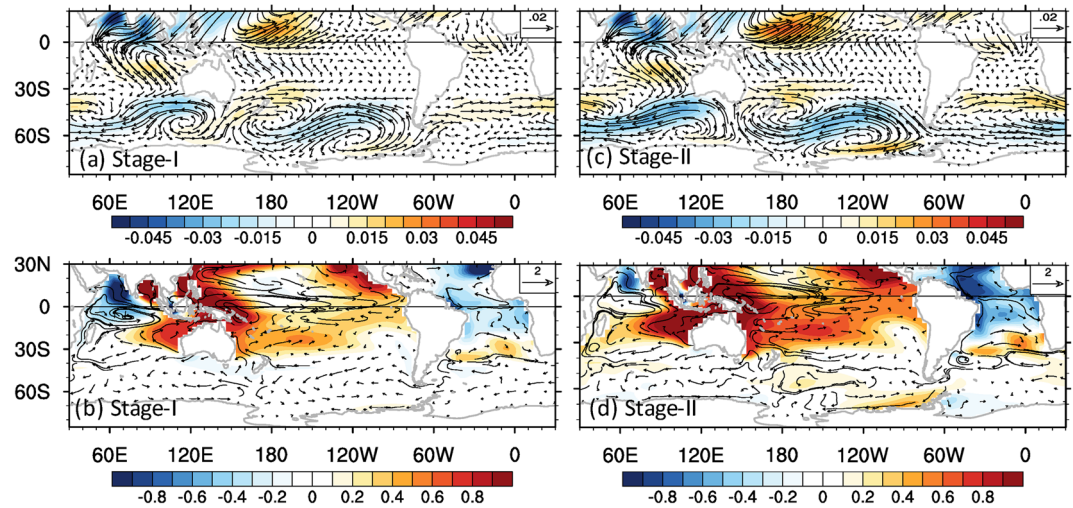
Wind stress, ocean current and salinity change

Figure 4. Changes in (a and c) ocean surface wind stress (vector; m/s) and zonal wind stress (shading; positive is for eastward anomaly; units: m/s) and (b and d) ocean surface current (vector; cm/s) and SSS (shading; psu). Left panel is for Stage-I and right panel is for Stage-II.

Although this a highly idealized modeling study, this work provides guidance regarding how the high mountains in the Northern Hemisphere affect the ocean circulation in the Southern Hemisphere, which has rarely been addressed in previous works. The unrealistic experiments can improve our understanding of detailed processes of the global impact of the TP since it is difficult to deduce the influence of mountain uplift on past climate change only from geological evidence. Our simulation also has potential implications for past climate change. For example, the Earth has experienced a long-term cooling trend throughout the Cenozoic (Zachos et al., 2008), with drastic decrease in atmospheric CO_2 since the Eocene (Cramer et al., 2009). This can be partially explained by weakened AABW in response to TP uplift, since the strong AABW before TP uplift can cause carbon release from deep ocean (Menviel et al., 2014).

The results obtained in our simulation is quite robust. For example, the atmospheric teleconnection between the tropical Indo-Pacific and Antarctic shows resemblance to prior works (Nuncio & Yuan, 2015). The intensified AABW in a world without the TP is also found in Su et al. (2018; their Figure 1h). Recently, we have run another three NoTP experiments starting from different initial conditions of CTRL. The AABW evolution is similar to the results in this study (Figure not shown). However, we admit that the conclusion drawn in this study are subject to experiment limitations. For example, the constant atmospheric CO_2 concentration (285 ppm) are used here, whereas it was much higher (up to 1,000 ppm) in the past warm word with limited sea-ice extent (Lowenstein & Demicco, 2006) and much higher sea level (Piper & Normark, 1989). The CO_2 and ice sheet extent can both affect AABW behaviors. Moreover, the topography configuration, such as open or closed Drake Passage, may cause important changes in SO circulation (Livermore et al., 2007) and thus the discrepancy of AABW response in our study from a paleo-topography viewpoint. Note that the AABW response in our study is not only caused remotely by the topography changes. Instead, it contains the contribution from thermal forcing over the TP since the TP removal also causes strong warming over there via lapse rate effect (Yang et al., 2020). In addition to experiment limitations, the model bias on the results in this work is another concern. The simulated excessive cold tongue in the eastern tropical Pacific in CESM (Yang et al., 2020) may exaggerate the ocean temperature response to surface forcings. The model resolutions for both ocean and atmosphere components are coarse; particularly, the ocean model used here cannot fully resolve the Antarctic polynyas, which may also trigger bias in AABW simulation (Weijer et al., 2017). Based on these limitations, one should bear in mind that the climate changes in response to sudden removal of the TP from the modern-day topography may not have to be consistent with the climate evolution with the gradual uplift of the TP during geological time. More coupled models with more deliberately designed experiments are extremely needed. How would the AABW be affected by

the uplift of the TP over the geological timescales associated with other major factors of the past tectonic changes? The answer would provide a greater mechanistic foundation for understanding the role of the TP in the long-term and climate changes in the past as well as implications to climate changes in the future.

Data Availability Statement

Data to produce the main figures in this paper can be found at: http://doi.org/10.5281/zenodo.4090944 and http://doi.org/10.5281/zenodo.4534389.

References

Adkins, J. F. (2013). The role of deep ocean circulation in setting glacial climates. *Paleoceanography*, *28*, 539–561. https://doi.org/10.1002/palo.20046

An, Z., Kutzbach, J., Prell, W., & Porter, S. (2001). Evolution of Asian monsoons and phased uplift of the Himalaya–Tibetan plateau since Late Miocene times. *Nature*, *411*(6833), 62–66. https://doi.org/10.1038/35075035

Boos, W., & Kuang, Z. (2010). Dominant control of the South Asian monsoon by orographic insulation versus plateau heating. *Nature*, *463*(7278), 218–222. https://doi.org/10.1038/nature08707

Cramer, B., Toggweiler, J., Wright, J., Katz, M., & Miller, K. (2009). Ocean overturning since the Late Cretaceous: Inferences from a new benthic foraminiferal isotope compilation. *Paleoceanography*, https://doi.org/10.1029/2008PA001683

Delworth, T. L., & Zeng, F. (2012). Multicentennial variability of the Atlantic meridional overturning circulation and its climatic influence in a 4000 year simulation of the GFDL CM2.1 climate model. *Geophysical Research Letters*, *39*(13). https://doi.org/10.1029/2012GL052107

Ding, Q., Steig, E. J., Battisti, D. S., & Kuttel, M. (2011). Winter warming in West Antarctica caused by central tropical Pacific warming. *Nature Geoscience*, *4*, 398–403. https://doi.org/10.1038/ngeo1129

Fallah, B., Cubasch, U., Prömmel, K., & Sodoudi, S. (2016). A numerical model study on the behaviour of Asian summer monsoon and AMOC due to orographic forcing of Tibetan Plateau. *Climate Dynamics*, *47*, 1485–1495. https://doi.org/10.1007/s00382-015-2914-5

Ferrari, R., Jansen, M. F., Adkins, J. F., Burke, A., Stewart, A. L., & Thompson, A. F. (2014). Antarctic sea ice control on ocean circulation in present and glacial climates. *Proceedings of the National Academy of Sciences of the United States of America*, *111*, 8753–8758. https://doi.org/10.1073/pnas.1323922111

Ganachaud, A., & Wunsch, C. (2001). Improved estimates of global ocean circulation, heat transport and mixing from hydrographic data. *Nature*, *408*, 453–457. https://doi.org/10.1038/35044048

Harrison, T., Copeland, P., Kidd, W., & Yin, A. (1992). Raising Tibet. *Science*, *255*(5052), 1663–1670.

Held, I. M., & Ting, M. (1990). Orographic versus thermal forcing of stationary waves: The importance of the mean low-level wind. *Journal of the Atmospheric Sciences*, *47*, 495–500. https://doi.org/10.1175/1520-0469(1990)047<0495:OVTFOS>2.0.CO;2

Hoskins, B. J., & Karoly, D. J. (1981). The steady linear response of a spherical atmosphere to thermal and orographic forcing. *Journal of the Atmospheric Sciences*, *38*, 1179–1196. https://doi.org/10.1175/1520-0469(1981)038<1179:TSLROA>2.0.CO;2

Hu, A., Meehl, G., Han, W., Otto-Bliestner, B., Abe-Ouchi, A., & Rosenbloom, N. (2015). Effects of the Bering Strait closure on AMOC and global climate under different background climates. *Progress in Oceanography*, *132*, 174–196.

Hunke, E. C., & Lipscomb, W. H. (2010). *CICE: The Los Alamos Sea Ice Model, documentation and software user's manual, version 4.1*. Los Alamos National Laboratory. LA-CC-06-012.Version 4.0

Hurrell, J. W., Holland, M. M., Gent, P. R., Ghan, S., Kay, J., Kushner, P. J., et al. (2013). The community earth system model: A framework for collaborative research. *Bulletin of the American Meteorological Society*, *94*, 1339–1360. https://doi.org/10.1175/BAMS-D-12-00121.1

Ito, T., & Marshall, J. (2008). Control of lower limb circulation in the Southern Ocean by diapycnal mixing and mesoscale eddy transfer. *Journal of Physical Oceanography*, *38*, 2832–2845. https://doi.org/10.1175/2008JPO3878.1

Jansen, M. F., & Nadeau, L. P. (2016). The effect of Southern Ocean surface buoyancy loss on the deep-ocean circulation and stratification. *Journal of Physical Oceanography*, *46*(11), 3455–3470. https://doi.org/10.1175/JPO-D-16-0084.1

Johnson, G. C. (2008). Quantifying Antarctic bottom water and North Atlantic deep water volumes. *Journal of Geophysical Research*, *113*(C5), C05027. https://doi.org/10.1029/2007 JC004477

Kamenkovich, I. V., & Goodman, P. J. (2000). The dependence of AABW transport in the Atlantic on vertical diffusivity. *Geophysical Research Letters*, *27*(22), 3739–3742. https://doi.org/10.1029/2000GL011675

Kitoh, A. (1997). Mountain uplift and surface temperature changes. *Geophysical Research Letters*, *24*, 185–188. https://doi.org/10.1029/96GL03953

Kouketsu, S., Doi, T., Kawano, T., Masuda, S., Sugiura, N., Sasaki, Y., et al. (2011). Deep ocean heat content changes estimated from observation and reanalysis product and their influence on sea level change. *Journal of Geophysical Research: Oceans*, *116*(C3). https://doi.org/10.1029/2010JC006464

Kutzbach, J. E., Guetter, P. J., Ruddiman, W. F., & Prell, W. L. (1989). Sensitivity of climate to late Cenozoic uplift in southern Asia and the American west: Numerical experiments. *Journal of Geophysical Research: Atmospheres*, *94*(D15), 18393–18407.

Lawrence, D. M., Oleson, K. W., Flanner, M. G., Fletcher, C. G., Lawrence, P. J., Levis, S., et al. (2012). The CCSM4 land simulation, 1850–2005: Assessment of surface climate and new capabilities. *Journal of Climate*, *25*(7), 2240–2260. https://doi.org/10.1175/JCLI-D-11-00103.1

Lowenstein, T., & Demicco, R. (2006). Elevated Eocene atmospheric CO_2 and its subsequent decline. *Science*, *313*(5795), 1928. https://doi.org/10.1126/science.1129555

Liu, W., & Fedorov, A. (2019). Global impacts of Arctic sea ice loss mediated by the Atlantic meridional overturning circulation. *Geophysical Research Letters*, *46*(2), 944–952. https://doi.org/10.1029/2018GL080602

Livermore, R., Hillenbrand, C., Meredith, M., & Eagles, G. (2007). Drake Passage and Cenozoic climate: An open and shut case?. *Geochemistry, Geophysics, Geosystems*, *8*(1), 1–11.

Lumpkin, R., & Speer, K. (2007). Global ocean meridional overturning. *Journal of Physical Oceanography*, *37*(10), 2550–2562. https://doi.org/10.1175/JPO3130.1

Marshall, G. J., Orr, A., van Lipzig, N. P. M., & King, J. (2006). The impact of a changing Southern Hemisphere annular mode on Antarctic Peninsula summer temperatures. *Journal of Climate*, *19*, 5388–5404. https://doi.org/10.1175/JCLI3844.1

Menviel, L., England, M. H., Meissner, K. J., Mouchet, A., & Yu, J. (2014). Atlantic-Pacific seesaw and its role in outgassing CO2 during Heinrich events. *Paleoceanography*, *29*(1), 58–70.

Molnar, P., England, P., & Martinod, J. (1993). Mantle dynamics, uplift of the Tibetan Plateau, and the Indian Monsoon. *Reviews of Geophysics*, *31*, 357–396. https://doi.org/10.1029/93RG02030

Nikurashin, M., & Vallis, G. (2011). A theory of deep stratification and overturning circulation in the ocean. *Journal of Physical Oceanography*, *41*(3), 485–502. https://doi.org/10.1175/2010JPO4529.1

Nuncio, M., & Yuan, X. (2015). The influence of the Indian Ocean dipole on Antarctic sea ice. *Journal of Climate*, *28*(7), 2682–2690. https://doi.org/10.1175/JCLI-D-14-00390.1

Park, S., Bretherton, C. S., & Rasch, P. J. (2014). Integrating cloud processes in the Community Atmosphere Model, version 5. *Journal of Climate*, *27*, 6821–6856. https://doi.org/10.1175/JCLI-D-14-00087.1

Pfister, P. L., Stocker, T. F., Rempfer, J., & Ritz, S. P. (2014). Influence of the Central American Seaway and Drake Passage on ocean circulation and neodymium isotopes: A model study. *Paleoceanography*, *29*(12), 1214–1237.

Piper, D., & Normark, W. (1989). Late Cenozoic sea-level changes and the onset of glaciation: Impact on continental slope progradation off eastern Canada. *Marine and Petroleum Geology*, *6*(4), 336–347.

Purich, A., & England, M. (2019). Tropical teleconnections to Antarctic sea ice during austral spring 2016 in coupled pacemaker experiments. *Geophysical Research Letters*, *46*(12), 6848–6858. https://doi.org/10.1029/2019GL082671

Purkey, S., & Johnson, G. (2013). Antarctic Bottom Water warming and freshening: Contributions to sea level rise, ocean freshwater budgets, and global heat gain. *Journal of Climate*, *26*(16), 6105–6122. https://doi.org/10.1175/JCLI-D-12-00834.1

Ruddiman, W. F., & Kutzbach, J. (1989). Forcing of Late Cenozoic Northern Hemisphere climate by plateau uplift in southern Asia and the American West. *Journal of Geophysical Research*, *94*, 18409–18427. https://doi.org/10.1029/JD094iD15p18409

Schmittner, A., Silva, T. A., Fraedrich, K., Kirk, E., & Lunkeit, F. (2011). Effects of Mountains and Ice Sheets on Global Ocean Circulation. *Journal of Climate*, *24*(11), 2814–2829. https://doi.org/10.1175/2010JCLI3982.1

Sebille, E., Spence, P., Mazloff, M. R., England, M. H., Rintoul, S. R., & Saenko, O. A. (2013). Abyssal connections of Antarctic Bottom Water in a Southern Ocean State Estimate. *Geophysical Research Letters*, *40*(10), 2177–2182. https://doi.org/10.1002/grl.50483

Shin, S. I., Liu, Z., Otto-Bliesner, B. L., Kutzbach, J. E., & Vavrus, S. J. (2003). Southern Ocean sea-ice control of the glacial North Atlantic thermohaline circulation. *Geophysical Research Letters*, *30*, 1096. https://doi.org/10.1029/2002GL015513

Sinha, B., Blaker, A. T., Hirschi, J., Bonham, S., Brand, M., Josey, S., et al. (2012). Mountain ranges favour vigorous Atlantic meridional overturning. *Geophysical Research Letters*, *39*(2), L02705(2). https://doi.org/10.1029/2011GL050485

Snow, K., Hogg, A., Sloyan, B., & Downes, S. M. (2016). Sensitivity of Antarctic Bottom Water to Changes in Surface Buoyancy Fluxes. *Journal of Climate*, *29*(1), 313–330. https://doi.org/10.1175/JCLI-D-15-0467.1

Stephens, B. B., & Keeling, R. F. (2002). The influence of Antarctic sea ice on glacial-interglacial CO_2 variations. *Nature*, *404*, 171–174. https://doi.org/10.1038/35004556

Stewart, A. L., Ferrari, R., & Thompson, A. F. (2014). On the importance of surface forcing in conceptual models of the deep ocean. *Journal of Physical Oceanography*, *44*, 891–899. https://doi.org/10.1175/JPO-D-13-0206.1

Su, B., Jiang, D., Zhang, R., Sepulchre, P., & Ramstein, G. (2018). Difference between the North Atlantic and Pacific meridional overturning circulation in response to the uplift of the Tibetan Plateau. *Climate Past*, *14*, 751–762. https://doi.org/10.5194/cp14-751-2018

Sun, S., Eisenman, I., & Stewart, A. L. (2016). The influence of Southern Ocean surface buoyancy forcing on glacial-interglacial changes in the global deep ocean stratification. *Geophysical Research Letters*, *43*, 8124–8132. https://doi.org/10.1002/2016GL070058

Talley, L. D. (2013). Closure of the global overturning circulation through the Indian, Pacific, and Southern Oceans: Schematics and transports. *Oceanography*, *26*(1), 80–97. https://www.jstor.org/stable/24862019

Turner, J. (2004). The El Nino-southern oscillation and Antarctica. *International Journal of Climatology: A Journal of the Royal Meteorological Society*, *24*(1), 1–31. https://doi.org/10.1002/joc.965

Wang, G., Hendon, H., Arblaster, J. M., Lim, E., Abhik, S., & Rensch, P. (2019). Compounding tropical and stratospheric forcing of the record low Antarctic sea-ice in 2016. *Nature communications*, *10*(1), 1–9. https://doi.org/10.1038/s41467-018-07689-7

Weijer, W., Veneziani, M., Stössel, A., Hecht, M., Jeffery, N., Jonko, A., et al. (2017). Local atmospheric response to an open-ocean polynya in a high-resolution climate model. *Journal of Climate*, *30*(5), 1629–1641. https://doi.org/10.1175/JCLI-D-16-0120.1

Wen, Q., & Yang, H. (2020). Investigating the role of the Tibetan Plateau in the formation of Pacific meridional overturning circulation. *Journal of Climate*, *33*(9), 3603–3617. https://doi.org/10.1175/JCLI-D-19-0206.1

Wu, G., Liu, Y., He, B., Bao, Q., Duan, A., & Jin, F. (2012). Thermal Controls on the Asian Summer Monsoon. *Science Report*, *2*(1), 1–7. https://doi.org/10.1038/srep00404

Yang, H., Li, Q., Wang, K., Sun, Y., & Sun, D. (2015). Decomposing the meridional heat transport in the climate system. *Climate Dynamics*, *44*(9-10), 2751–2768. https://doi.org/10.1007/s00382-014-2380-5

Yang, H., & Wen, Q. (2020). Investigating the role of the Tibetan Plateau in the formation of Atlantic meridional overturning circulation. *Journal of Climate*, *33*(9), 3585–3601. https://doi.org/10.1175/JCLI-D-19-0205.1

Zachos, J. C., Dickens, G., & Zeebe, R. (2008). An early Cenozoic perspective on greenhouse warming and carbon-cycle dynamics. *Nature*, *451*(7176), 279–283. https://doi.org/10.1038/nature06588

Zhang, L., Delworth, T. L., & Jia, L. (2017). Diagnosis of decadal predictability of Southern Ocean sea surface temperature in the GFDL CM2. 1 model. *Journal of Climate*, *30*(16), 6309–6328. https://doi.org/10.1175/JCLI-D-16-0537.1

Zhou, X., Zhao, P., Chen, J., Chen, L., & Li, W. (2009). Impacts of thermodynamic processes over the Tibetan Plateau on the Northern Hemispheric climate. *Science in China Series D: Earth Sciences*, *52*(11), 1679–1693.

Zhu, J., Liu, Z., Zhang, J., & Liu, W. (2015). AMOC response to global warming: dependence on the background climate and response timescale. *Climate Dynamics*, *44*(11-12), 3449–3468. https://doi.org/10.1007/s00382-014-2165-x

References From the Supporting Information

Hieronymus, M., & Nycander, J. (2013). The budgets of heat and salinity in NEMO. *Ocean Modelling*, *67*, 28–38. https://doi.org/10.1016/j.ocemod.2013.03.006

Pond, S., & Pickard, G. (1983). *Introductory dynamical oceanography*. Gulf Professional Publishing.

Talley, L. D. (2011). *Descriptive physical oceanography: An introduction*. Academic Press.